# Nanocrystallization by current annealing (with and without tensile stress) of $Fe_{73.5-x}Ni_xSi_{13.5}B_9Nb_3Cu_1$ alloy ribbons ($x = 5$, 10, and 20)

Cite as: J. Appl. Phys. **103**, 113904 (2008); https://doi.org/10.1063/1.2937201
Submitted: 27 June 2007 . Accepted: 09 April 2008 . Published Online: 06 June 2008

**N. Iturriza, N. Murillo, J. J. del Val, J. González, G. Vara, and A. R. Pierna**

# Nanocrystallization by current annealing (with and without tensile stress) of $Fe_{73.5-x}Ni_xSi_{13.5}B_9Nb_3Cu_1$ alloy ribbons ($x$=5, 10, and 20)

N. Iturriza,[1,2] N. Murillo,[2] J. J. del Val,[1,3] J. González,[1,a)] G. Vara,[4] and A. R. Pierna[4]
[1]*Department of Materials Physics, Faculty of Chemistry, UPV/EHU, P° Manuel de Lardizabal 3, 20018 San Sebastián, Spain*
[2]*New Materials Department, CIDETEC, P° Miramón 196, 20.009-San Sebastián, Spain*
[3]*Unidad de Física de Materiales, Centro Mixto CSIC-UPV/EHU, 20018 San Sebastián, Spain*
[4]*Departamento de Ingeniería Química y Medio Ambiente, Escuela Universitaria Politécnica, UPV/EHU Plaza Europa s/n, 20018 San Sebastián, Spain*

(Received 27 June 2007; accepted 9 April 2008; published online 6 June 2008)

Microstructural (crystalline volume fraction and grain size), magnetization (coercive field), and saturation magnetostriction measurements in $Fe_{73.5-x}Ni_xSi_{13.5}B_9Nb_3Cu_1$ alloy ribbons ($x$=5, 10, and 20) treated by current annealing and stress-current annealing are presented. Microstructural analysis of the treated ribbons using x-ray diffraction showed a high content of the amorphous phase in the bulk. In addition, substantial changes in the crystalline state such as grain size of the samples annealed at different conditions were observed. The alloy composition also affects greatly the grain size: increase in Ni content leads to higher values of the average grain size. The evolutions of the coercive field with the two kinds of thermal treatment were analyzed, allowing us to conclude that the addition of Ni tends to reduce the magnetic softness of the original material and that the coercivities are higher in the samples treated by stress annealing than in those treated without tensile stress. On the other hand, the saturation magnetostriction decreases with the thermal treatment, which is in agreement with the microstructural behavior (structural relaxation and nanocrystallization process), although some discrepancies are found for samples with $x$=5. © *2008 American Institute of Physics*. [DOI: 10.1063/1.2937201]

## I. INTRODUCTION

Recently, promising iron-based nanocrystalline alloys with improved magnetic softness comparing to that of the precursor amorphous material have been developed. Most of the investigations aimed at achieving optimal soft magnetic properties deal with a typical $Fe_{73.6}Cu_1Nb_3Si_{13.5}B_9$ composition (trademark Finemet) with a nanocrystalline grain structure produced by the partial devitrification of the precursor amorphous as-cast sample.[1–9] A small amount of Cu atoms, acting as nucleation centers for crystallites, and of Nb atoms, preventing the grain growth, are crucial for the formation of nanoparticles. After the first stage of crystallization, Fe(Si) crystallites are finely dispersed in the residual amorphous matrix. The soft magnetic behavior of these Fe-based nanocrystalline alloys is due to the following two effects: the first one is the correlation exchange length, which is larger than the grain size, and the second one is the opposite sign of the magnetostriction constant of the crystallites and of the residual amorphous matrix, allowing a reduction in the average magnetostriction. Although optimum soft magnetic properties of the melt-spun amorphous alloys were usually obtained after stress-relief annealing, it was widely believed that the magnetic softness of any amorphous alloy deteriorates by increasing the annealing temperature far beyond the crystallization temperature. Nevertheless, this conclusion was found to be not generally correct. Yoshizawa *et al.*[1] reported in 1988 that the magnetic softness of melt-spun amorphous Finemet was improved significantly by a careful annealing treatment leading to primary crystallization of fine $\alpha$-Fe(Si) grains of an average size of around 10 nm and 70% of relative volume fraction randomly dispersed in the residual amorphous matrix. The alloy exhibited in the nanocrystalline states an exceptionally high effective permeability ($\mu_e$) value of the order of $10^5$, with a quite high saturation magnetization ($M_s$) of 1.25 T at room temperature, and nearly zero effective saturation magnetostriction ($\lambda_s$). This improved magnetic softness is originated by the formation of a unique microstructure composed of fine grains (with a size of about 10 nm).

On the other hand, the soft magnetic behavior of these nanocrystalline alloys has been satisfactorily explained by considering the two-phase character of such materials. Thus, in accordance with these ideas, the variation of the magnetic properties, denoted by $X$, owing to the thermal treatment was considered in terms of the relative volume percentage of the crystalline phase (usually $\alpha$-FeSi) and the residual amorphous matrix, e.g.,

$$X = \nu_D X^{\mathrm{cr}} + (1 - \nu_D) X^{\mathrm{am}}, \tag{1}$$

where $\upsilon_D$ is the volume fraction of the nanograins.[10] It is assumed that spherical shapes for such grains and $X$ stands for the saturation magnetostriction constant ($\lambda_S$) or the saturation magnetization ($M_S$).

In a previous work,[11] we have reported on the microstructural changes in $Fe_{73.5-x}Ni_xSi_{13.5}B_9Nb_3Cu_1$ amorphous alloy ribbons ($x$=5, 10, and 20) induced by two thermal

a)Author to whom correspondence should be addressed. Electronic mail: wapgoesj@sc.ehu.es.

 

treatments (using the Joule heating with and without tensile stress) in order to elucidate the complex magnetic behavior which can be expected at the surface of the ribbons. Thus, the measurement of the surface hysteresis loops reveals much higher coercive field values than those obtained in the bulk material. In this work, we present new interesting results of the effect of the substitution of Fe atoms by Ni in the classical Finemet composition, which are mainly related to the bulk coercive field and saturation magnetostriction parameters.

## II. EXPERIMENTAL

Amorphous alloy ribbons with the nominal compositions $Fe_{73.5-x}Ni_xSi_{13.5}B_9Nb_3Cu_1$ ($x=5$, $x=10$, and $x=20$) of approximately 3 mm wide and 20 $\mu$m thick were prepared by a melt-spinning technique. The noncrystalline character of the as-quenched ribbons was confirmed by x-ray diffraction (XRD) and transmission electron microscopy (TEM) analyses.

Thermal treatments of the as-quenched ribbons were carried out by means of Joule-heating technique[12] different times up to 60 min. The current density of about 40 40 A/mm$^2$ was found to be optimal for achieving the largest nanocrystalline volume fraction. In all subsequent measurements, this current density value was fixed. One set of samples was annealed under simultaneously applied an external tensile stress (95 MPa), which was kept during the subsequent cooling down to room temperature. The samples treated with stress annealing are referred to as SA samples. The other set of samples underwent the same annealing process without the application of the external tensile stress; they are referred to as CA samples and used for comparison with the corresponding SA samples. The fluxmetric measurements carried out on the treated samples have evidenced the presence of an induced anisotropy, revealing very different shapes of the hysteresis loops depending on the applied thermal treatment.

The structural analysis of the ribbons in bulk was carried out by XRD method. The XRD measurements were made with a powder diffractometer (with an automatic divergence slit and a monochromator) using Cu $K\alpha$ wavelength of 0.15 nm. The patterns obtained were normalized in the high $q$ range ($q \geqslant 40$ nm$^{-1}$) where the intensity did not vary for different samples owing to the very short structural distances responsible for the scattering in this region. As the treated samples reveal a semicrystalline behavior with an amorphous halo and crystalline peaks overlapped in the diffraction pattern, the crystalline phase amount ($\chi$) is obtained from the area of the crystalline peak relative to the total area where the peak appears. In order to get the two contributions separated, the experimental peak was fitted to a sum of a Gaussian function (corresponding to the crystalline peak) and a Lorentzian function (corresponding to the amorphous halo)[11,12] (see Fig. 1). The average size of the crystallites ($D$) was evaluated from Scherrer's formula using the Gaussian function deducted from the fitting.[12,13]

The coercive field of the samples was evaluated from the hysteresis loops obtained by a fluxmetric method in the range of 20–300 Hz. The extrapolation to zero frequency allowed deducing the coercivity representative of the bulk in quasistatic conditions.[12] The saturation magnetization for these samples has been accurately measured in a number of works[14] and the cited values are 1.39, 1.14, and 0.95 T for $x=5$, 10, and 20, respectively.

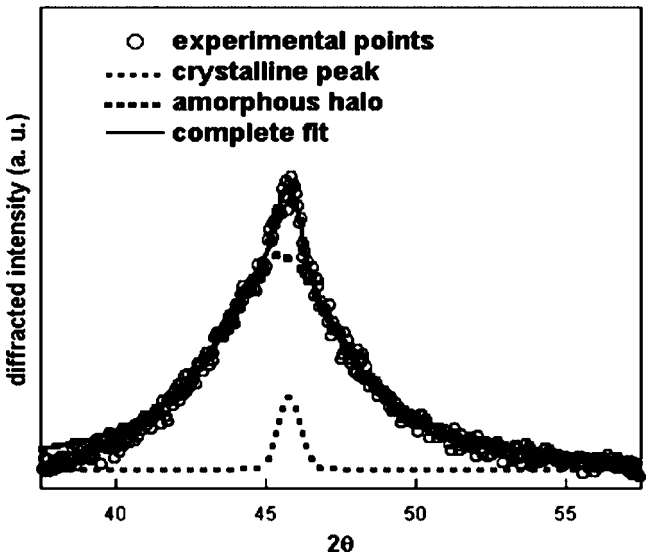


FIG. 1. Example of the separation of the crystalline and amorphous contributions in a given XRD peak.

Saturation magnetostriction measurements have been carried out by the small angle magnetization rotation (SAMR) technique.[15–17] As detailed elsewhere,[15] the method makes use of the variation in the signal $V_{2\omega}$, picked up by a narrow coil when applying simultaneously to the sample a saturating dc axial field $H_z$, a small transverse field $H_y$, and one tensile stress $\sigma_a$. When a tensile stress $\sigma_a$ is applied, the induced signal $V_{2\omega}$ measured by a lock-in amplifier, increases or decreases as a consequence of the increment of the magnetoelastic anisotropy with a transverse or longitudinal easy axis, respectively. This change in $V_{2\omega}$ can be compensated by an adequate modification of $H_z$ so that $V_{2\omega}$ takes the same value as that before the stress was applied. In this way, the saturation magnetostriction coefficient, $\lambda_S$, is obtained as

$$\lambda_S = -(\mu_0 M_S/3)[\Delta H/\Delta\sigma_a]_{V_{2\omega}=\text{constant}}, \quad (2)$$

where $\mu_0 M_S$ is the saturation magnetization of the sample

## III. EXPERIMENTAL RESULTS AND DISCUSSION

### A. XRD analysis

From the XRD measurements in the CA and SA samples as commonly practiced, the fractional volume of the crystalline phase and the average grain size of crystals were evaluated. Figure 2 shows the fractional crystalline volume of the CA and SA samples, respectively, as a function of the annealing time in the different Ni-Finemet samples. For a short time (2 min) the crystallites were not observed in the CA samples while the crystallization seems to start at the very beginning of annealing for SA samples, indicating that the presence of tensile stress assists the nanocrystallization process in the similar way to that observed in Co-Finemet

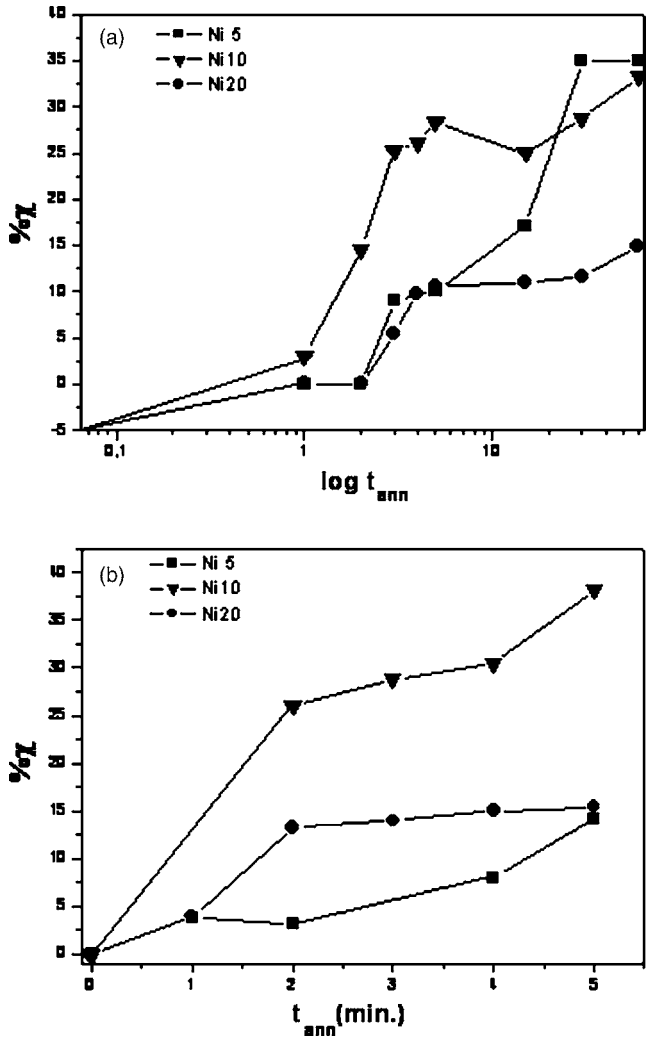


FIG. 2. Evolution of the partial crystallization volume with the annealing time: (a) CA treated samples; (b) SA treated samples.

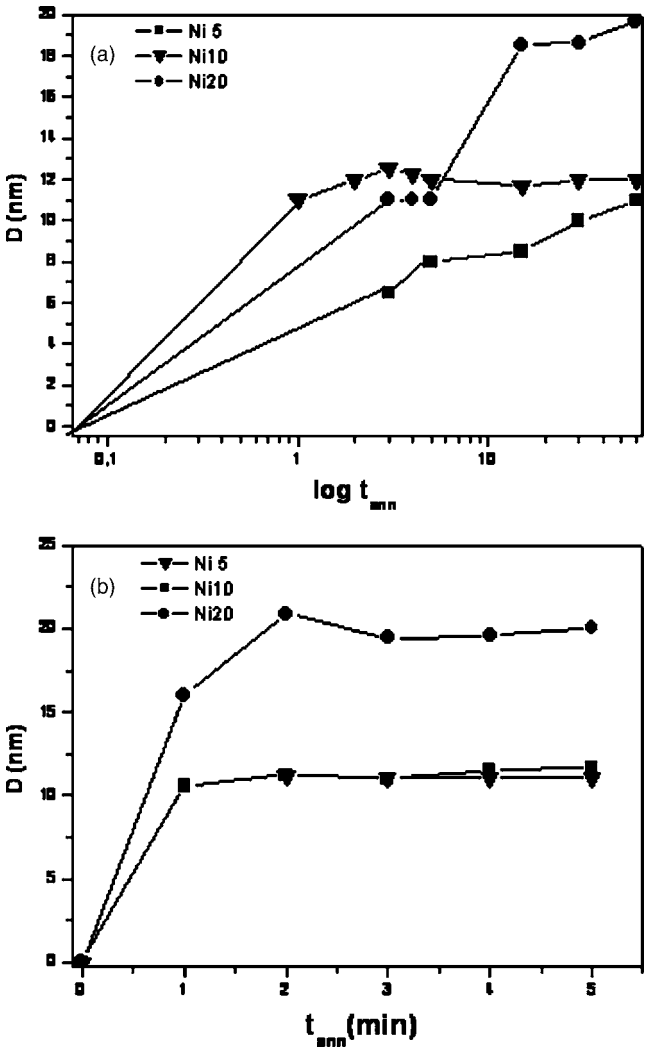


FIG. 3. Evolution of the average grain size ($D$) with the annealing time: (a) CA treated samples; (b) SA treated samples.

samples.[12] As it is expected, the fraction of crystalline volume increases with the annealing time, this increase being more significant as the Ni content becomes greater. It must be noted that the crystalline volume fraction values obtained with these treatments are clearly lower (70%–80%) than those in samples treated by conventional annealing (using a furnace) with annealing parameters of 550 °C, 1 h.[1] Therefore, it appears that the current annealing technique does not allow a similar percentage of the nanocrystalline fraction to be achieved as in classical Finemet alloys, probably because of the kinetics associated with the current annealing. This is certainly a disadvantage, as it is well known that the current annealing procedure is more convenient due to its high heating rate and less complexity by avoiding the use of a furnace. Moreover, the degree of magnetic softness which can be achieved in nanocrystalline alloys treated by current annealing is quite similar to that when the same nanocrystalline alloy is treated by conventional annealing.[9]

Figure 3 shows the evolution of the average grain size of the CA and SA samples, respectively. The average grain size $D$ increases with the annealing time up to the sizes ($D_{sat}$) of around 10, 15, and 20 nm for $x=5$, 10, and 20, respectively. These sizes, $D_{sat}$, are the same for the CA and SA samples, although the kinetics of segregation of such grains is different as it can be observed in Fig. 4 where the variations of the average grain size with the two treatments in each composition are shown. It can be seen that for all three compositions, the saturation value of $D$ with the annealing time is reached faster in SA samples comparing to CA samples. In addition, according to our work and previous x-ray and TEM analysis,[11,18] these nanocrystalline Ni-Finemet alloys contain supersaturated phases of $\alpha$-Fe(Si), $Fe_3Si$; Ni rich and $Fe_3NiSi_{1.5}$ which play a very important role in the magnetostrictive behavior. Obviously, the segregation of Ni rich and $Fe_3NiSi_{1.5}$ is more significant as the Ni content increases.

### B. Coercivity behavior

Figure 5 shows the hysteresis loops of the as-quenched, CA, and SA treated samples of the alloy with $x=5$ annealed for 5 min. As a general feature, a very low value of the coercive field in all three samples can be observed. It is noted that the inclination of the hysteresis loops of the treated samples (mainly for SA ones) corresponds to a transversely induced macroscopic anisotropy. The origin of such anisotropy could be the pair magnetic ordering for the CA samples

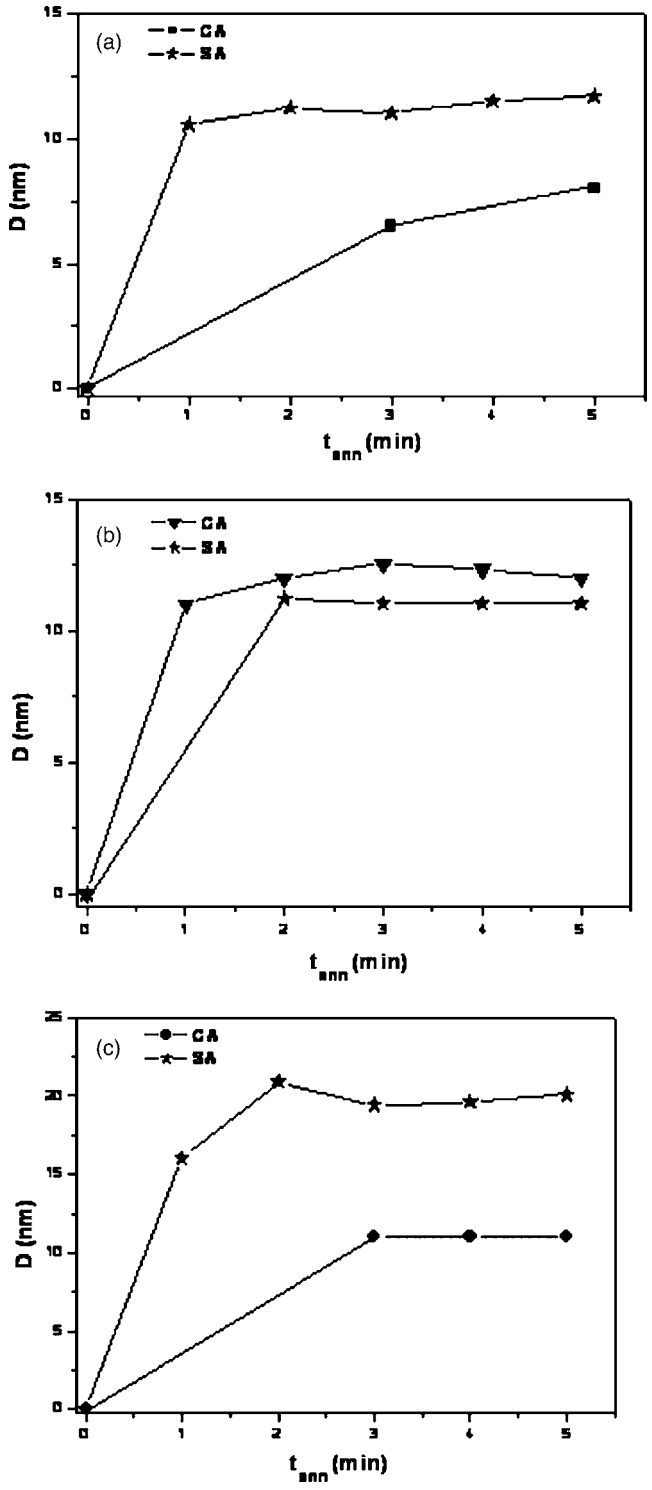


FIG. 4. Comparison of the variation of $D$ with the CA and SA treatments in the compositions (a) $x=5$, (b) $x=10$, (c) and $x=20$.

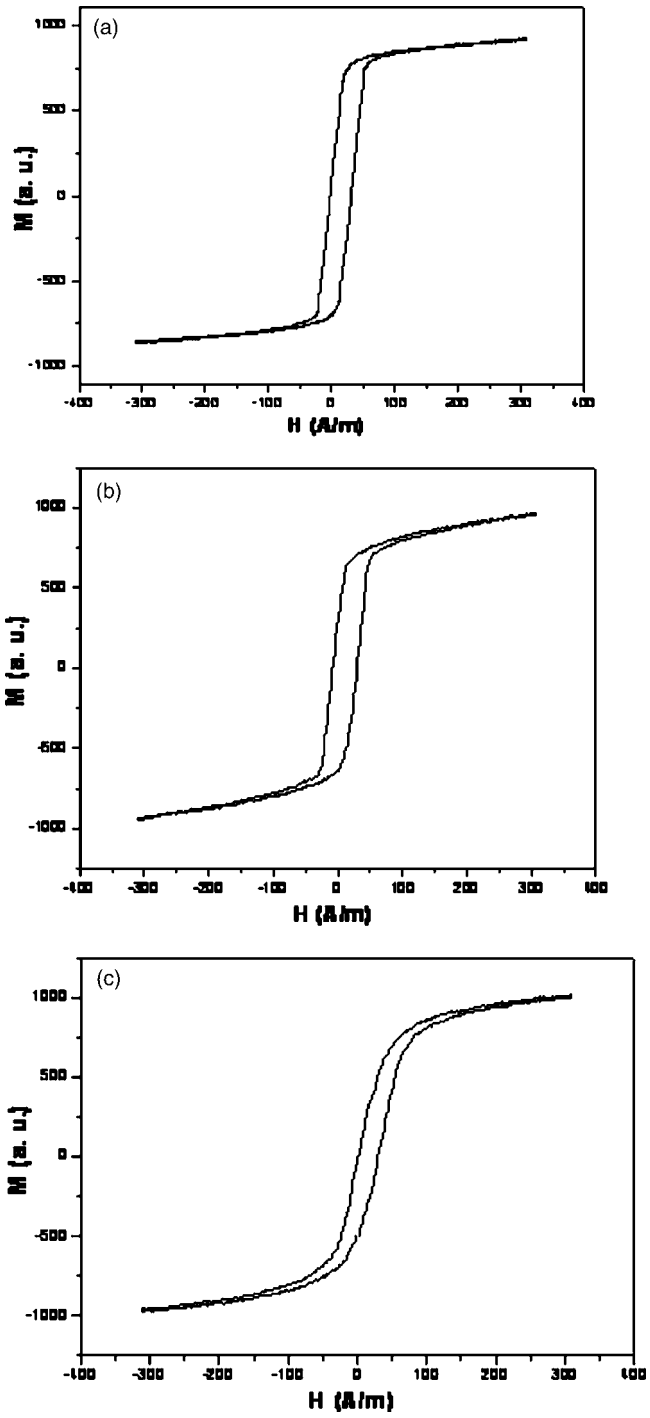


FIG. 5. Hysteresis loops of the (a) as-quenched, (b) CA treated, and (c) SA treated $x=5$ alloy.

(since CA is equivalent to a transverse field annealing),[19] while in the case of SA sample, such origin is more complicated.[12,20,21]

The variations in the coercive field ($H_C$) as a function of the annealing time in CA and SA samples of the Ni-Finemet alloys are presented in Fig. 6. The CA treatment reduces the $H_C$ value, but not down to the level about $H_C \approx 1$ A/m obtained in the classical Finemet. This difference was ascribed to the effect of the induced anisotropy (e.g., shape, magnetoelastic and stress, or field induced anisotropies[19,22]) on the coercivity, which could be quite significant in the case of a random magnetocrystalline anisotropy. Moreover, as it can be expected, $H_C$ values of the SA alloys are larger than those in CA alloys, which could be understood as a consequence of a larger transverse magnetic anisotropy induced by the SA treatment.

After the first step of crystallization, FeSi crystallites are finely dispersed in the residual amorphous matrix. In a wide range of crystallized volume fraction, the exchange correlation length is larger than the average intergranular distance $d$

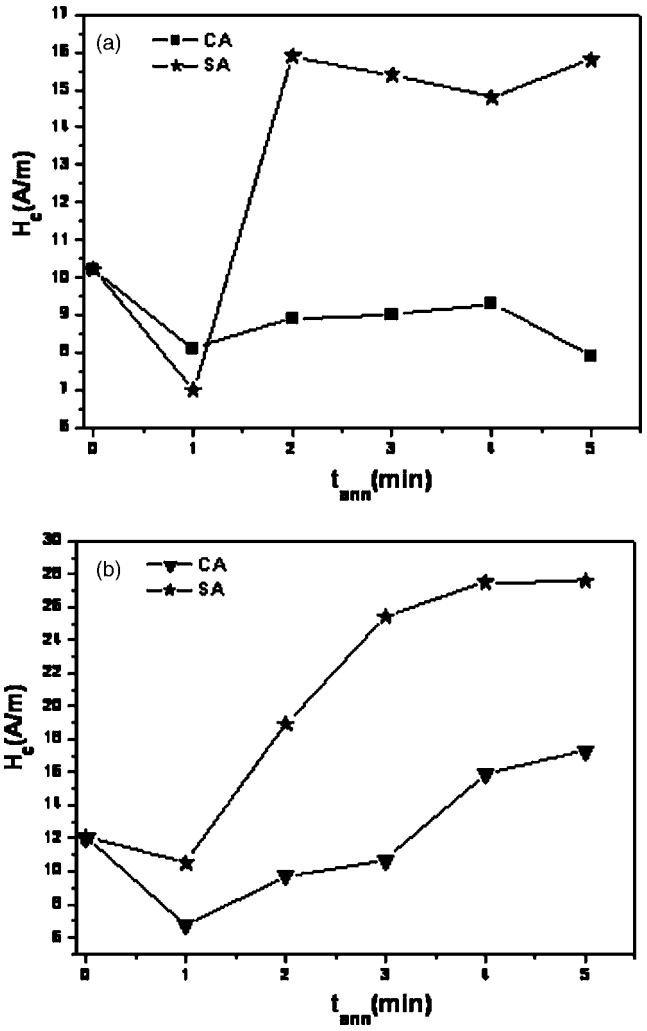


FIG. 6. Variations of the coercive field with the CA and SA treatments in the composition (a) $x=5$ and (b) $x=10$.

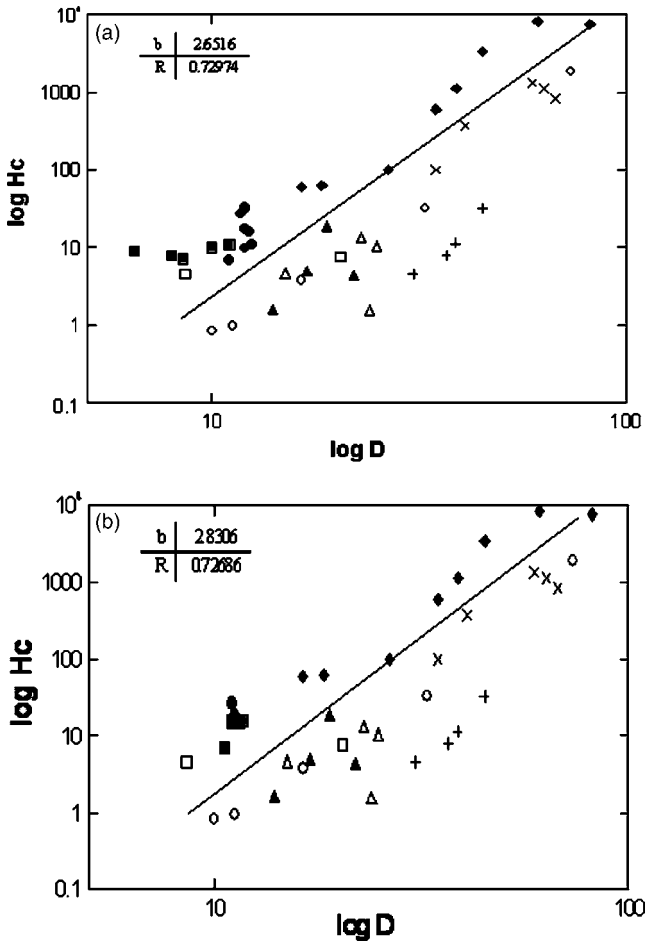


FIG. 7. Dependencies of the coercivity with the grain size for several nanocrystalline alloys: (a) samples nanocrystallized by conventional furnace and Ni-Finemet submitted to CA treatment, (b) conventional annealing and Ni-Finemet submitted to SA treatment, (■) Ni5-Finemet, (●) Ni10-Finemet, (○) FeCuNbSiB, (×) FeNbSiB, (△) FeCuTaSiB, (▲) FeCuSiB, (+) FeCuVSiB, (□) FeZrB, and (♦) FeZrCo.

and the exchange correlation length of the grains is larger than the grain size $D$. The magnetic softness of the Fe-rich nanocrystalline phase is partly due to the following reason: the opposite signs of the magnetostriction constant for the crystallites and for the residual amorphous matrix, which allow a reduction in the average magnetostriction.

On the other hand, considering that the grain size $D$ is smaller than the exchange length $L_{ex}$ and that the nanocrystals are fully coupled, the random anisotropy model implies a dependence of the effective magnetic anisotropy, $\langle K\rangle$, on the sixth power of the average grain size $D$. The coercivity is understood as a coherent rotation of the magnetic moments of each grain toward the effective axis, leading to the same dependence of the coercivity with the grain size,[2] where the coercive field is given by the expression

$$H_C = p_c[\langle K\rangle/J_S] = p_c\{K_1^4 D^6/J_S A^3\} \quad \text{with } \langle K\rangle = (K_1^4 D^6/A^3), \tag{3}$$

where $K_1=8$ kJ/m$^3$ is the magnetocrystalline anisotropy of the grains, $A=10^{-11}$ J/m is the exchange ferromagnetic constant, $J_S=1.2$ T is the saturation magnetic polarization, and $p_c$ is a dimensionless prefactor close to the unity.

The predicted $D^6$ dependence of the coercivity has been widely accepted to be followed in a $D$ range below $L_{ex}$ (around 35–40 nm) for nanocrystalline Fe–Si–B–M–Cu ($M$ =IV A and VI A metal) alloys.[4,23] We have plotted in Fig. 7 the coercive field versus the grain size of several compositions (FeCuNbSiB, FeNbSiB, FeCuTaSiB, FeCuSiB, FeCuVSiB, FeZrB, FeZrCo) reported in the literature[2,9,23–28] together with those obtained in the CA and SA alloys of this work. As it can be seen, a clear deviation from the predicted $D^6$ law is observed similarly to that reported in Refs. 6 and 9. Thus, the experimental results reported here, as well as those in Ref. 9, show that $H_C$ versus $D$ obeys a $D^3$ law. Deviations from the $D^6$ law were also reported by Suzuki *et al.*[23] and ascribed to the role of an induced anisotropy. Indeed, it is not reasonable to assume that the only source of anisotropy is the one arising from the different crystalline nanoparticles (mentioned previously), since other sources of anisotropy seem to be not realistic (dipolar interactions have some relevance, see Ref. 29). In fact, CA treatment is equivalent to an annealing under the action of a transverse magnetic field and, consequently, it can induce an inhomogeneous transverse anisotropy,[19] while SA can induce a more homogeneous transverse anisotropy. Nevertheless, both kinds of anisotro-

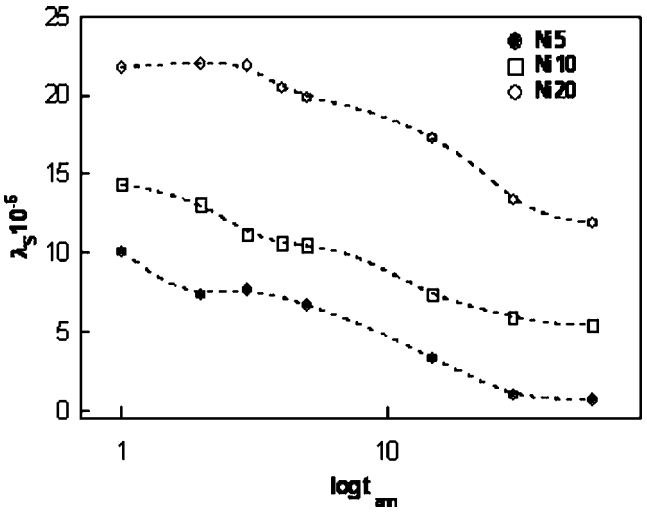


FIG. 8. Evolution of the effective saturation magnetostriction constant ($\lambda_S^{eff}$) with the annealing time in the CA Ni-Finemet alloys.

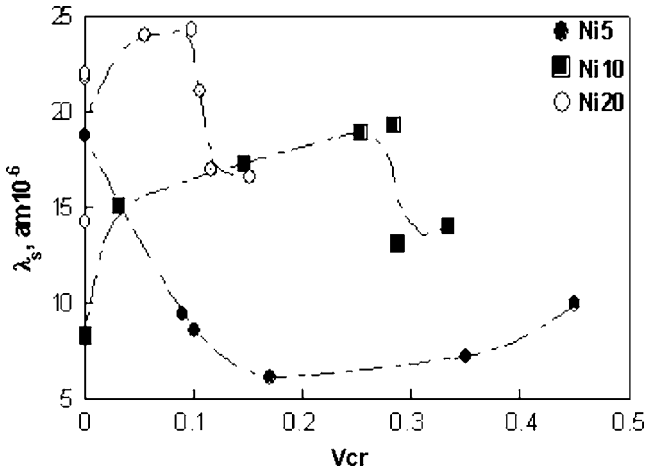


FIG. 9. Evolution of the saturation magnetostriction constant of the residual amorphous matrix ($\lambda_S^{am}$) with the crystalline volume fraction in the CA Ni-Finemet alloys.

pies contribute similarly to the $H_C(D)$ dependencies. Therefore, types of annealings used in this work could induce inhomogeneous magnetic anisotropy, which could be responsible for this significant change in the coercive field dependence on the grain size. As a consequence, the presence of longer-range uniaxial anisotropies larger than the averaged magnetocrystalline anisotropies $\langle K_1 \rangle$ and, hence, the reduction in $H_C$ is not detected as in the case of the Finemet alloy. Additionally, it should also be noted that the occurrence of dipolar and deteriorated exchange intergrain interaction can, interestingly, account for the substitution of Fe by Ni atoms.

### C. Saturation magnetostriction behavior

Experimental results for $\lambda_S$ in the CA samples are presented as a function of the annealing time in Fig. 8. As it can be seen, $\lambda_S$ decreases with the Ni content in the as-quenched and treated samples. This fact should be attributed to the transformation of the amorphous state into a nanocrystalline one and the resulting $\lambda_S$ is affected by the magnetostriction of the forming nanocrystalline grains with different chemical compositions. Thus, $\lambda_S$ increases slightly for short annealing times and decreases monotonously with the annealing time for the $x=5$ sample while, on the contrary, for the $x=10$ and $x=20$ samples, $\lambda_S$ increases for short annealing time (in connection with a structural relaxation[30]), and then decreases for long annealing time when the nanocrystallization occurs, in the same way that has been observed in the classical Finemet alloy. Therefore, in the course of structural relaxation, $\lambda_S$ after initial moderate increase decreases in the initial stages of crystallization where the transformation of quenched-in cluster structures into phases with lower Si content [$\alpha$-Fe and $\alpha$-Fe(Si)]takes place.[9,31] As a consequence, the initial increases in $\lambda_S$ observed in the $x=5$ sample (similarly to that previously observed for $x=0$) could indicate an activation of clusters with a short-range ordering and a composition probably rich in metalloid atoms. For longer annealing times, it is reasonable to assume a higher concentration of Si atoms in the bcc-Fe or even the saturated $Fe_3Si$ phase in both cases with a negative saturation magnetostriction, which leads to a decrease in the effective magnetostriction ($\lambda_S^{eff}$).

As it has been mentioned, the primary crystallization in these Fe-rich samples gives rise to a single phase $\alpha$-Fe(Si), $Fe_3Si$ Ni-rich, and $\alpha$-$Fe_3NiSi_{1.5}$ crystallites embedded in the amorphous residual matrix depleted in the Fe content. According to Ref. 10, the experimental data of the effective saturation magnetostriction ($\lambda_S$) of the nanocrystalline alloy, [$\alpha$-Fe(Si)] ($\lambda_S^{cr}$) (Ref. 32) are negative depending on the Si atoms. Negative character of the saturation magnetostriction is reported elsewhere[18,33] for $Fe_3Si$ and Ni-rich grains with values of $-9\times10^{-6}$ and $-30\times10^{-6}$, respectively, while $Fe_3NiSi_{1.5}$ is nonmagnetostrictive. It must be noted that the magnetostriction of a residual amorphous alloy ($\lambda_S^{am}$) can be assumed to be positive. Therefore, the crystalline grains and the residual amorphous matrix have the saturation magnetostriction with different signs, negative for the nanocrystals and positive for the amorphous matrix. In this way, we have estimated the term corresponding to the residual amorphous matrix in Eq. (1) as a function of the partial crystalline fraction (Fig. 9). The decrease in $\lambda_S^{am}$ in the $x=5$ sample with partial crystalline volume seems to be in contradiction with the expected increase probably due to the residual amorphous matrix poor in Si atoms. In the case of the $x=10$ and $x=20$ samples, the initial increase in $\lambda_S^{am}$ could be associated with possible invar effect[34] because the segregation of Ni-rich grains with a large value of negative magnetostriction ($-30\times10^{-6}$) (Ref. 33) implies a large positive magnetostriction of the residual amorphous matrix in accordance with the effective magnetostriction values measured in these nanocrystalline alloys.

New efforts have been made, recently, to explain these discrepancies. In this context, an additional contribution arising from the boundary grains has been taken into account for the analysis of the effective magnetostriction, as was proposed in an additional contribution similarly to that reported in Refs. 35 and 36. In this way, a surface contribution for the effective saturation magnetostriction may be derived according to,

$$\lambda_S^{\text{eff}} = p\lambda_S^{\text{cr}} + (1-p)(\lambda_S^{\text{am}} + kp) + \pi\lambda_S^s(S/V), \quad (4)$$

where $k$ is a parameter which expresses the changes in the magnetostriction in the residual amorphous phase with the evolution of the crystallization process. The last term describes the effects of the interfaces and depends on the surface to volume $(S/V)$ ratio for individual grains, as well as on the surface magnetostriction constant $\lambda_S^s$, which characterizes the crystal-amorphous interface.

Therefore, Eq. (4) could be considered as the basic relationship that can be used to understand the experimental data on the effective magnetostriction in Fe-based nanocrystalline alloys at different stages of crystallization. Assuming a spherical form of grains, (two kinds of grains, as previously mentioned) with radius $R$, the last term of Eq. (4) can be expressed as $3\lambda_S^s/R$ and the magnetostriction constant which describes the interface $\lambda_S^s$ can be estimated. For these Ni-Finemet alloys, the average value of $R$ is about 10 nm and, thus, $\lambda_S^s$ has been found to vary in the range of $10^{-6}$ nm,[37] which is one order of magnitude smaller than the values for the surface magnetostriction reported in multilayer systems. Consequently, the value $\lambda_S^s$ estimated in these nanocrystalline alloys is within the range of the surface magnetostriction for thin iron layers.

## IV. CONCLUSIONS

Current annealing (with or without tensile stress) treatments performed in Ni-Finemet ribbons produce macroscopic changes (structural relaxation followed by the nanocrystallization process) which modify the magnetic (coercive field) and magnetoelastic (saturation magnetostriction constant) behavior of the ribbons. In the present work, we have reported such changes analyzing the effect of the substitution of Fe by Ni in the classical Finemet composition. In addition, two kinds of thermal treatments lead to some differences in the coercivity of the samples. The use of a tensile stress is found to activate the nucleation rate, while grains with a reduced grain size compared to that of standard ribbons are found. The saturation magnetostriction measurements reveal the influence of the Ni content because the structural relaxation effect appears to be absent in the $x=5$ alloy. The additive character of the effective magnetostriction arising from the partial volume of the two phases (crystals and residual amorphous matrix) in the nanocrystalline samples is indicative of a third contribution of surface character (contribution arising from the boundary grains) which should be taken into account. Nevertheless, the aspects related to the structure and properties of the surface grain boundaries as well as the local strains which can affect the magnetoelastic interactions in the crystal-remaining amorphous matrix still need to be better investigated to understand the soft magnetic behavior exhibited by these nanocrystalline Fe-based alloys.

## ACKNOWLEDGMENTS

The authors are deeply acknowledge to Professor L.V. Panina (University of Plymouth, UK) for her kindly assistance. This work has been supported by the Basque Country Government and the Excma Diputación Foral de Gipuzkoa under the project NANOTRON.

[1] Y. Yoshizawa, S. Oguma, and K. Yamauchi, J. Appl. Phys. **64**, 6044 (1988).
[2] G. Herzer, IEEE Trans. Magn. **Mag-26**, 1397 (1990).
[3] N. Müller and N. Mattern, J. Magn. Magn. Mater. **136**, 79 (1994).
[4] G. Herzer, Scr. Metall. Mater. **33**, 1713 (1995).
[5] A. Hernando and M. Vázquez, in *Rapidly Solidified Alloys*, edited by H. H. Liebermann (Dekker, New York, 1993), p. 553.
[6] A. Hernando, M. Vázquez, T. Kulik, and C. Prados, Phys. Rev. B **51**, 3581 (1995).
[7] A. Hernando, P. Marín, M. Vázquez, J. M. Barandiarán, and G. Herzer, Phys. Rev. B **58**, 366 (1998).
[8] J. M. González, C. de Julián, F. Cebollada, A. K. Giri, and J. González, J. Appl. Phys. **81**, 4658 (1997).
[9] N. Murillo and J. González, J. Magn. Magn. Mater. **218**, 53 (2000).
[10] J. González, Appl. Phys. Lett. **85**, 5944 (2004).
[11] N. Iturriza, L. Fernández, A. Chizhik, G. Vara, A. R. Pierna, and J. J. del Val, J. Nanosci. Nanotechnol. (in press).
[12] C. Miguel, A. P. Zhukov, J. J. del Val, A. Ramírez de Arellano, and J. González, J. Appl. Phys. **97**, 034911 (2005).
[13] N. Iturriza, C. García, L. Fernández, J. J. del Val, J. González, J. M. Blanco, G. Vara, and A. R. Pierna, J. Appl. Phys. **99**, 08F104 (2006).
[14] P. Aguado and M. Vázquez, J. Appl. Phys. **97**, 023901 (2005).
[15] K. Narita, J. Yamasaki, and H. Fukunaga, IEEE Trans. Magn. **Mag-16**, 435 (1980).
[16] A. Hernando, M. Vázquez, V. Madurga, E. Ascasibar, and M. Liniers, J. Magn. Magn. Mater. **61**, 39 (1986).
[17] J. M. Blanco, L. Domínguez, P. Aragoneses, and J. González, J. Magn. Magn. Mater. **186**, 135 (1998).
[18] G. Vlasák, P. Svec, and D. Janickovic, Mater. Sci. Eng., A **375–377**, 1149 (2004).
[19] M. Vázquez, J. González, and A. Hernando, J. Magn. Magn. Mater. **53**, 323 (1986).
[20] M. Ohnuma, K. Hono, T. Yanai, H. Fukunaga, and Y. Yoshizawa, Appl. Phys. Lett. **83**, 2859 (2003).
[21] B. Hoffmann and H. Kronmüller, J. Magn. Magn. Mater. **152**, 91 (1996).
[22] J. González, M. Vázquez, J. M. Barandiarán, V. Madurga, and A. Hernando, J. Magn. Magn. Mater. **68**, 151 (1987).
[23] K. Suzuki, G. Herzer, and M. Cadogan, J. Magn. Magn. Mater. **177**, 949 (1998).
[24] C. Miguel, N. Murillo, and J. Gonzalez, J. Appl. Phys. **88**, 6623 (2000).
[25] N. Murillo, J. Gonzalez, F. Cebollada, and J. M. González, Mater. Sci. Forum **269–272**, 865 (1998).
[26] T. Sawa and Y. Takahashi, J. Appl. Phys. **67**, 5565 (1990).
[27] K. Suzuki, A. Makino, N. Kataoka, A. Ionue, and T. Masumoto, J. Appl. Phys. **70**, 6232 (1991).
[28] H. Q. Guo, T. Reininger, H. Kronmüller, M. Rapp, and V. H. Skoumryev, J. Magn. Magn. Mater. **112**, 287 (1992).
[29] J. M. González, N. Murillo, J. González, J. M. Blanco, and J. Echeberria, J. Mater. Res. **11**, 512 (1996).
[30] M. A. Escobar, A. R. Yavari, E. T. de Lacheisserie, and J. González, Mater. Sci. Eng., A **133**, 184 (1991).
[31] M. Vázquez, P. Marin, A. O. Olofinjana, and H. A. Davies, Appl. Phys. Lett. **64**, 3184 (1994).
[32] T. Yamamoto, *Development of Sendust* (Komiyama, Chiba, 1980), p. 22.
[33] E. Du Tremolet de Lacheisserie, *Magnetostriction: Theory and Applications of Magnetoelasticity* (CRC, Roca Raton, FL, 1993).
[34] K. Shirakawa, S. Ohnuma, M. Nose, and T. Masumoto, IEEE Trans. Magn. **Mag-16**, 910 (1980).
[35] A. Slawska-Waniewska and R. Zuberek, J. Magn. Magn. Mater. **160**, 253 (1996).
[36] A. Slawska-Waniewska, R. Zuberek, J. González, and H. Szymczak, Mater. Sci. Eng., A **226–228**, 220 (1997).
[37] R. Zuberek, H. Szymczak, H. Krishnan, C. Sela, and M. Kaabouchi, J. Magn. Magn. Mater. **121**, 510 (1993).